Available online at www.sciencedirect.com
ScienceDirect
Dyes and Pigments 78 (2008) 157–164
DYES and PIGMENTS
www.elsevier.com/locate/dyepig

Malayaite ceramic pigments prepared with galvanic sludge

G. Costa [a], M.J. Ribeiro [a], J.A. Labrincha [b,*], M. Dondi [c], F. Matteucci [c], G. Cruciani [d]

[a] *UIDM, ESTG, Polytechnic Institute of Viana do Castelo, 4900 Viana do Castelo, Portugal*
[b] *Ceramics and Glass Engineering Department, CICECO, University of Aveiro, 3810-193 Aveiro, Portugal*
[c] *Istituto di Scienza e Tecnologia dei Materiali Ceramici, CNR-ISTEC, 48018 Faenza, Italy*
[d] *Department of Earth Sciences, University of Ferrara, 44100 Ferrara, Italy*

Received 24 May 2007; received in revised form 15 November 2007; accepted 19 November 2007
Available online 26 November 2007

Abstract

The synthesis and characterisation of chrome-tin red malayaite $Ca(Cr,Sn)SiO_5$ pigments are reported. The novel approach of using a galvanizing sludge from the Cr/Ni plating process as colouring agent is investigated. The ceramic pigments were prepared using a common, solid state reaction process, with optimisation of milling and firing conditions. Characterisation was undertaken using X-ray powder diffraction, diffuse reflectance spectroscopy and application in standard ceramic glazes. The ceramic pigments were of high purity (≥96% malayaite) and developed a burgundy colour due to the occurrence of Cr^{4+} and Cr^{3+} and also Ni^{2+} in the sludge-bearing samples. The hue of the pigments agreed with standard expectations and optimal formulations showed better performance than some commercial pigments, perhaps due to the contribution of nickel.

Keywords: Industrial Cr/Ni galvanizing sludge; Malayaite; Ceramic pigments; Recycling; Optical spectroscopy

1. Introduction

Cr-doped materials have been widely investigated as ceramic pigments. Depending on the synthesis conditions, Cr ions might assume different oxidation states (II–IV) leading to different colours and variable degrees of stability [1]. Pink chromium-doped malayaite $Ca(Sn,Cr)SiO_5$ is among the most important chromium pigments used in the ceramic industry for colouring glazes and it is catalogued under number 12-25-5 in the DCMA classification [2]. Nowadays these pigments are the main alternative to cadmium-containing pigments in the pottery industry, offering stability until 1300 °C [3]. However, some fundamental aspects associated with these pigments, such as the metal oxidation state, the localization and distribution of chromium species in the sphene lattice, are still under debate [4].

The preparation and characterisation of this type of chromium-containing pigment have been studied by different authors [5–7]. The sphene structure can be described to be composed of chains of corner-sharing SnO_6 octahedra running parallel to the cell edges that are cross-linked by silicate tetrahedra to form a $SnOSiO_4$ framework that accommodates Ca^{2+} in irregular hepta-coordinated polyhedra [5]. The crystallochemistry of sphene structures indicates that the chromium cations in both structures are in octahedral sites, substituting Sn^{4+} ions. Recent works concluded that in the Cr-doped sphene structure most of the tetravalent chromium cations form a solid solution with the sphene lattice by mostly Sn^{4+} substitution in octahedral positions, while a very small amount of Cr^{4+} might also substitute for Si^{4+} ions [8,9]. The small amount of chromium used imposes extra difficulties with respect to distinguishing between different oxidation states [5,6].

In the ceramic industry, natural and synthetic pigments find applications as colouring agents in glasses, enamels and unglazed bodies. Currently, synthetic ceramic inorganic pigments are prepared and widely used for the production of

* Corresponding author. Tel.: +351 234370250; fax: +351 234370204.
E-mail address: jal@ua.pt (J.A. Labrincha).

0143-7208/$ - see front matter © 2007 Elsevier Ltd. All rights reserved.
doi:10.1016/j.dyepig.2007.11.004

Table 1
Pigments' formulations (wt%) and corresponding codes: S1 means "standard" or fully obtained from solely commercial reagents, attempting to reproduce (molar%) the M1 waste-containing pigment

Sample	Formulations (wt%)					Cr_2O_3/SnO_2
	G-s	$CaCO_3$	SiO_2	SnO_2	Cr_2O_3	
S1	–	31.6	19.0	47.5	1.7	0.036
M1	10.8	28.7	17.2	43.3	–	0.036
M2	6.2	30.2	18.1	45.5	–	0.020
M3	5.2	30.5	18.3	46.0	–	0.016
M4	1.7	31.6	19.0	47.7	–	0.005

coloured glazed and unglazed tiles [10]. There has been a great interest in the ceramic industry for developing high stable pigments that show intense tonalities and that comply with technological and environmental demands [11]. One of the current trends is the search for alternative and less expensive raw materials. Selected industrial wastes have been investigated for this purpose [12,13]. In fact, industrial processes like powder surface coating or Cr/Ni plating consume large amounts of water. A huge flow of wastewater that is produced needs to be treated, yielding large amounts of normally hazardous sludge [14]. As part of searching for waste reuse alternatives, we have tried to prepare new ceramic pigments obtained by solid state reactions of mixtures composed of several industrial wastes [13,15], such as the actual Cr/Ni coating sludge. The main focus of the current work is on the synthesis of chrome-tin red malayaite $Ca(Cr,Sn)SiO_5$ pigment, incorporating Cr/Ni plating sludge as relevant components.

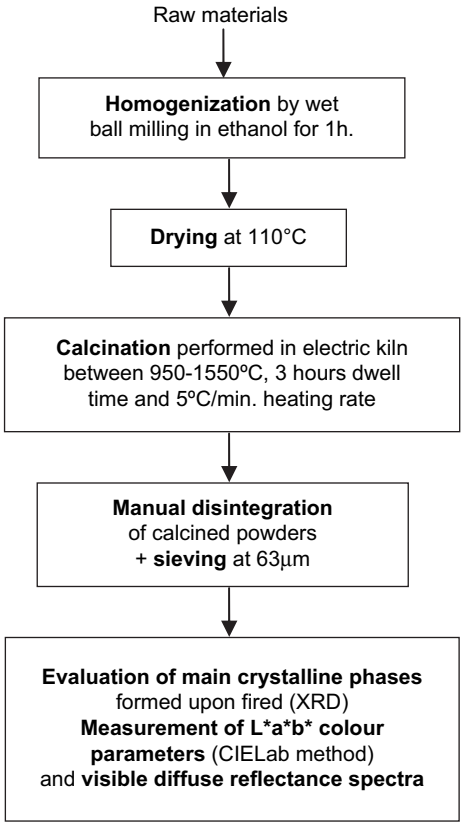

Fig. 1. Schematic representation of preparation and characterisation steps of the pigments.

2. Experimental

2.1. Raw materials and formulations

The waste consists of a galvanizing sludge from the Cr/Ni plating process (G-s). It was used after disintegration and drying at 100 °C. The characterisation included determinations of chemical composition (XRF, Philips X'UNIQUE II), thermal behaviour (DTA and TGA, Netzsch, STA 409EP) and particle size distribution (SediGraph 5100 V3.2). Crystalline phases were identified by X-ray diffraction (XRD, Rigaku Geigerflex D/max-Series). Calcite (Calcitec M1), Silica sand (Sibelco P500), and SnO_2 (CCT, MP 989) were also used in the synthesis batches. The starting batch formulations are shown in Table 1. For comparison purposes, a standard formulation (quoted as S1) fully obtained from solely commercial reagents, was also prepared. In this case, Cr_2O_3 (Merck, Selectipur) was used instead of sludge as a source for chromium.

2.2. Preparation and characterisation of pigments

In order to obtain fine and homogeneous slurries, mixtures were ball-milled in ethanol for 1 h. The as-prepared suspensions were dried at 110 °C and then calcined in an electric kiln at temperatures varying between 1250 and 1550 °C (3 h dwell time and 5 °C/min. heating/cooling rate). Calcined powders were manually disaggregated and sieved below 63 μm. Fig. 1 gives a schematic representation of all these steps.

A preliminary characterisation of pigments involved the identification (by XRD) of the main crystalline phases formed, upon firing, and measurements of the CIE Lab colour parameters. This method uses the reflectance data in the visible region to obtain the three relevant parameters, L^*, a^*, b^*, measuring the brightness, red/green and yellow/blue hue intensities,

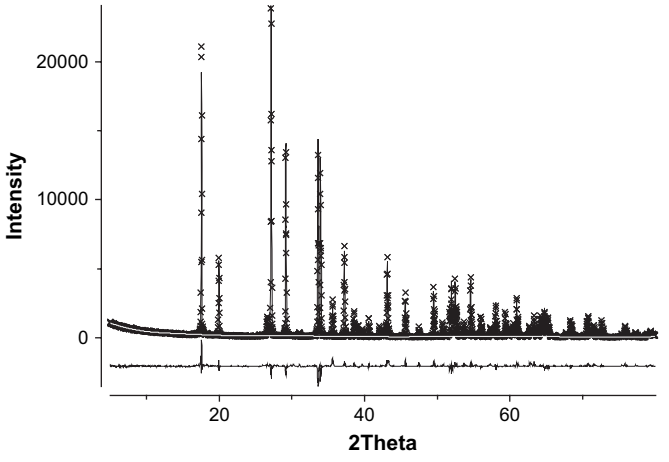

Fig. 2. Rietveld refinement plot of the X-ray powder diffraction data of sample S1. In the figure the continuous line represents the calculated pattern, while cross-points show the observed pattern. The difference curve between observed and calculated profiles is plotted below.

Table 2
X-ray diffraction data: refinement parameters, phase composition and unit cell parameters

Parameters (unit)	S1	M1	M2	M3	M4
GOF					
Rp_w (%)	9.9	17.1	11.6	13.7	10.2
$R\ \|F^2\|$ (%)	6.4	7.8	10.2	9.7	6.4
QPA					
Malayaite (wt%)	97.5(2)	97.0(2)	98.0(2)	97.7(2)	96.6(2)
Cassiterite (wt%)	2.5(2)	3.0(2)	2.0(2)	2.3(2)	3.4(2)
Malayaite					
a (Å)	7.1503(1)	7.1474(1)	7.1494(1)	7.1488(1)	7.1493(1)
b (Å)	8.8934(1)	8.8894(1)	8.8918(1)	8.8898(2)	8.8911(1)
c (Å)	6.6676(1)	6.6648(1)	6.6662(1)	6.6657(1)	6.6664(1)
b (°)	113.34(1)	113.33(1)	113.33(1)	113.33(1)	113.33(1)
Volume (Å^3)	389.32(1)	388.84(1)	389.12(1)	388.98(2)	389.10(1)
SnO_2					
$a = b$ (Å)	4.7369(3)	4.7360(2)	4.7371(4)	4.7360(6)	4.7368(2)
c (Å)	3.1832(4)	3.1849(3)	3.1848(5)	3.1811(7)	3.1851(3)
Volume (Å^3)	71.43(1)	71.44(2)	71.47(2)	71.35(2)	71.47(1)

Figures in parentheses are standard deviations in the last decimal figure.

respectively [16]. The visible diffuse reflectance spectra of the pigments were recorded on a Jasco V-560 UV–vis spectrophotometer, using MgO as reference. XRD data for Rietveld refinements were collected by a Bruker D8 Advance diffractometer, equipped with a Si(Li) solid state detector (Sol-X), using Cu Kα radiation. Rietveld refinements of X-ray diffraction patterns were performed using the GSAS and EXPGUI softwares [17,18]. Thirty-two independent variables were refined: scale-factors, zero-point, 15 coefficients of the shifted Chebyschev function to fit the background, unit cell dimensions, profile coefficients (1 Gaussian, G_W, and 2 Lorentzian terms, L_x and L_y). An example of Rietveld refinement is plotted in Fig. 2 while the figures-of-merit obtained are listed in Table 2.

Diffuse reflectance spectroscopy (DRS) was performed with a Perkin Elmer λ35 spectrophotometer in the 300–1100 nm range (0.03 nm step) using $BaSO_4$ integrating sphere and white reference material. Reflectance (R_∞) was converted to absorbance (K/S) by the Kubelka–Munk equation: $K/S = 2(1-R_\infty)\cdot 2R_\infty^{-1}$ [19,20]. Energy, full width at half maximum (FWHM) and intensity of the main absorbance bands in the optical spectra were determined through a deconvolution procedure (PFM, OriginLab).

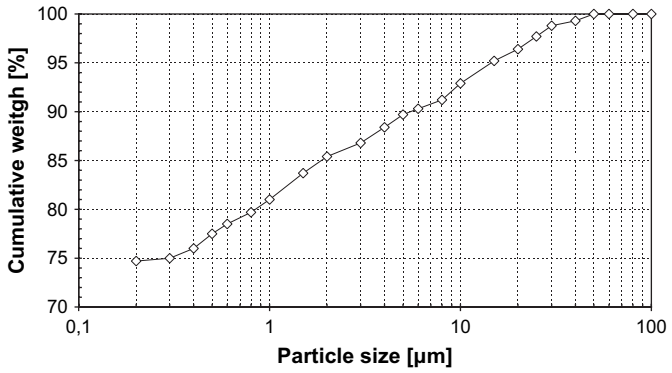

Fig. 3. Particle size distribution of the dried G-s.

The particle size distribution of the pigments in the as-used condition was also determined.

Finally, each pigment was added (5 wt%) to a transparent and bright lead-free commercial glaze (SiO_2, Al_2O_3, B_2O_3, CaO as main constituents plus 2–8% Na_2O, and <2% K_2O) and to an opaque and bright commercial glaze (SiO_2, B_2O_3, ZrO_2 as main constituents plus 2–8% Al_2O_3, Na_2O, CaO, and <2% K_2O, MgO, and ZnO). The mixtures were ball-milled in ethanol for 15 min and were dried at 110 °C. The powders were then used to press buttons ($\phi = 2.5$ cm) that were fired at 1050 °C (30 min dwell time and 5 °C/min heating rate) in an electric furnace. Their final colour was evaluated in the same way as already described.

3. Results and discussion

3.1. Waste characterisation

G-s is produced by the physico-chemical treatment of wastewaters generated by a Ni/Cr plating plant. The possible chemical composition variability requires careful sampling and homogenising procedures to assure reasonable constancy [21]. This sludge is mostly composed of metal hydroxide gels, sulphate salts and occasionally chlorides. The main metal species are combined forming nitrogen, oxygen, hydrogen, sulphur and carbon-containing compounds. Once properly sampled and homogenised, the average chemical composition in (wt%): 0.23 Al_2O_3, 0.53 Fe_2O_3, 33.17 NiO, 14.49 Cr_2O_3, 3.15 SiO_2, 0.60 CaO, 1.41 Na_2O, 2.13 ZnO, 0.86 SO_4, 6.33 other components and 37.10 loss of ignition at 1000 °C.

Fig. 3 shows the cumulative particle size distribution curve of the dried and disintegrated sludge. Particles are finer than 40 μm while the average diameter is below 0.2 μm.

This sludge was partially dried by exposure in open air conditions. Then, its thermal behaviour was studied by DTA/TGA. The total weight loss reaches 45% (dry basis). Major

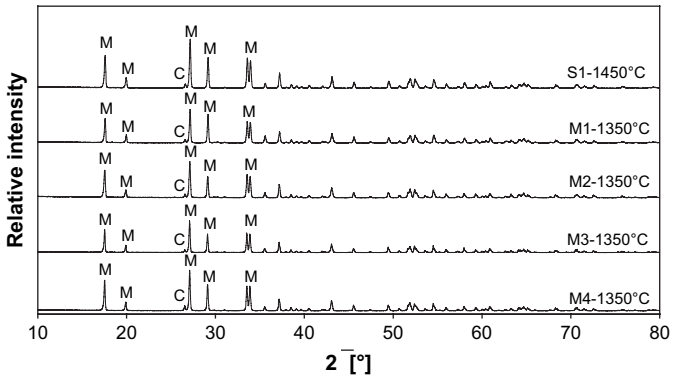

Fig. 4. XRD patterns of powdered pigments: S1 calcined at 1450 °C, M1, M2, M3 and M4 calcined at 1350 °C. The following phases were identified: Malayaite = M; Cassiterite = C.

decomposition reactions occur up to about 500 °C, confirming that hydroxide gels are the main constituents of the sludge. Reactions observed at higher temperatures (650–700 °C) are due to decomposition of sulphates/chlorides. The XRD pattern of G-s powder after calcination at 950 °C reveals the following phases: nickel–chromium spinel $NiCr_2O_4$, olivine Ni_2SiO_4, nickel oxide NiO, zinc oxide ZnO, and quartz SiO_2. More details of sludge characteristics are given elsewhere [21].

3.2. Pigment preparation and characterisation

Table 1 lists the four malayaite formulations prepared. S1 and M1 pigments have a Cr_2O_3:SnO_2 molar ratio = 0.036, as suggested by Lopez-Navarrete et al. [4]. In order to explore other hues, M2, M3, and M4 pigments (Cr_2O_3:SnO_2 = 0.03, 0.01, and 0.005, respectively) were also prepared. The use of sludge implied the simultaneous introduction of nickel; the NiO:SnO_2 molar ratio is as high as 0.167, 0.091, 0.076 and 0.024 for the samples M1, M2, M3 and M4, respectively.

XRD refinements of pigments show malayaite as the major phase (Table 2 and Fig. 4). However, approximately 2–3% of SnO_2 (cassiterite) is present in all formulations, denoting that

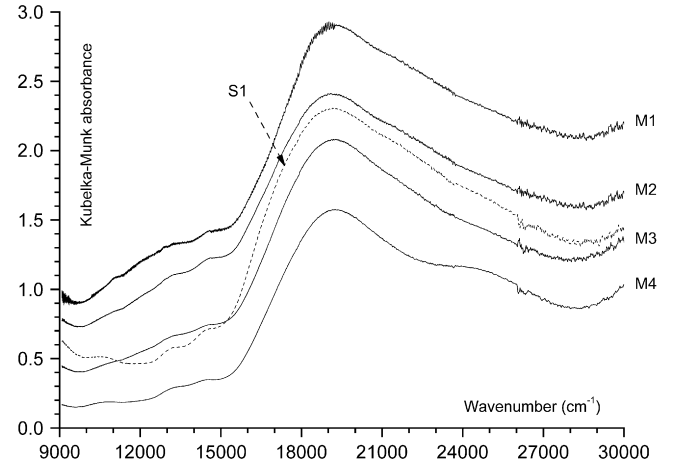

Fig. 5. Diffuse reflectance spectra of malayaite pigments.

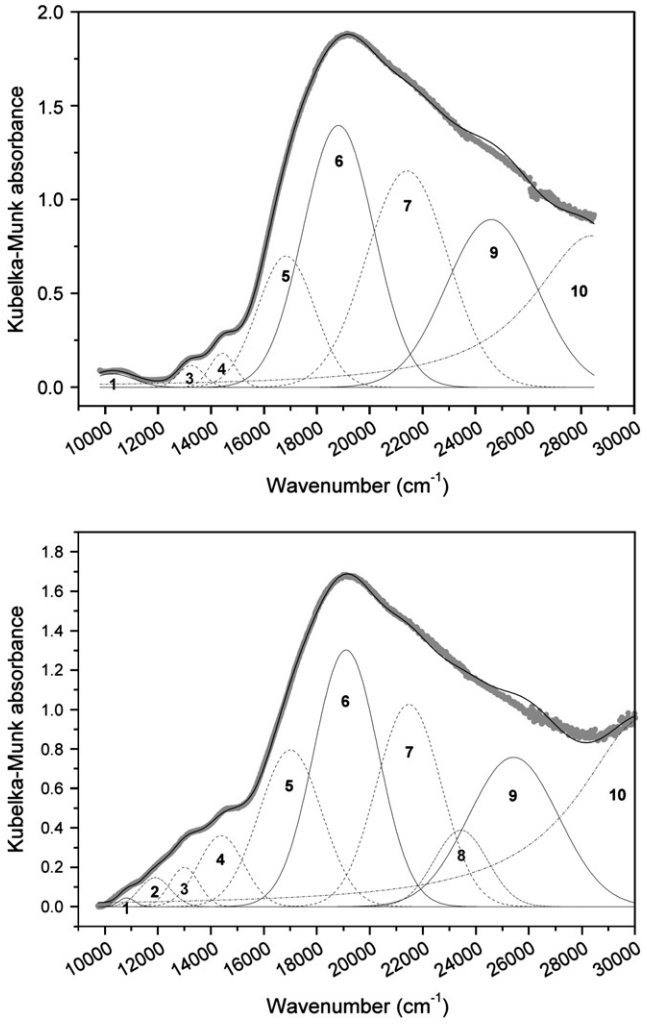

Fig. 6. Deconvolution of diffuse reflectance spectra of S1 (above) and M3 (below). The bands are numbered with reference to Table 3.

reaction between the components was not complete, as commonly happens in industrial conditions. As expected, enhancing the firing temperature improves the reactivity and as a consequence the amounts of unreacted components tend to diminish. However, there is evidence that the degree of purity of malayaite is not a crucial requisite to obtain an intense pink colour [22].

The unit cell dimensions of the reference Cr-doped malayaite are close to the literature values, as are those of cassiterite [4,18]. In contrast, the use of sludge as colouring agent induces a slight contraction of the malayaite unit cell (Table 2), perhaps due to the additional effect of other transition elements (e.g. Ni) added along with Cr.

Cr-doped malayaite has been considered for a long time as a solid solution pigment. There has been some controversy in the literature in assigning the oxidation states and coordination geometries of chromium ions in this pigment. Although recent studies suggest that chromium ions might also occupy tetrahedral sites, there is general agreement that most of the chromium assumes an octahedral coordination, substituting Sn^{4+} cations [5,6].

Table 3
Optical spectroscopic data of malayaite pigments

Ion (ground state)	Transition	Band	S1			M1			M2			M3			M4		
			Peak	FWHM	Area	Peak	FWHM	Area	Peak	FWHM	Area	Peak	FWHM	Area	Peak	FWHM	Area
Cr^{4+}, $^3T_{1g}(^3F)$	$^1E_g + {}^1T_{2g}(^1D)$	1	10,270	1970	108	10,980	1000	105	10,820	720	34	11,000	1640	128	10,800	2290	164
	$^3T_{2g}(^3F)$	6	18,820	3140	4668	19,050	3090	5500	19,100	2860	3969	19,250	3090	4466	19,130	3260	4252
	$^3T_{1g}(^3P)$	9	24,590	4000	3763	25,590	4000	4145	25,420	3990	3217	25,340	4000	2697	25,880	4000	2397
Cr^{3+}, $^4A_{2g}(^4F)$	$^2E_g(^2G)$	3	13,250	1130	141	13,280	1330	375	13,000	1280	272	13,060	1290	229	13,150	1110	133
	$^2T_{1g}(^2G)$	4	14,430	1130	219	14,490	1570	505	14,390	2008	771	14,350	1860	514	14,320	1620	305
	$^4T_{2g}(^4F)$	5	16,840	2530	1886	16,780	3020	2080	17,000	2780	2350	17,140	2910	2218	17,020	2800	1365
	$^4T_{1g}(^4F)$	7	21,420	3620	4441	21,390	2640	3055	21,470	2870	3140	21,520	2680	2359	21,460	2880	1960
Ni^{2+}, $^3A_{2g}(^3F)$	$^3T_{1g}(^3F)$	2	–	–	–	12,160	1510	395	11,900	1380	217	12,080	1230	132	12,220	1190	58
	$^3T_{1g}(^3P)$	8	–	–	–	23,260	2620	1935	23,430	2370	980	23,340	2630	1256	23,600	3230	1946

The bands are numbered with reference to Fig. 6.

Table 4
CIE Lab colour coordinates (L^*, a^*, b^*) for the sintered pigments and buttons (glaze + 5 wt% of pigment) fired at 1050 °C

Sample	Temp. (°C)	CIE Lab parameter								
		Pigment			Transparent glaze			Opaque glaze		
		L^*	a^*	b^*	L^*	a^*	b^*	L^*	a^*	b^*
S1	1250	64.7	+10.1	+4.6	–	–	–	–	–	–
	1350	49.5	+18.0	+3.8	44.1	+13.7	+5.4	75.8	+7.8	+1.4
	1450	35.2	+24.2	+4.8	36.6	+16.6	+3.3	65.5	+12.5	+0.4
	1550	28.7	+20.1	+3.1	35.3	+14.5	+2.4	68.2	+9.9	−0.5
M1	1350	27.1	+12.9	+0.9	34.5	+9.5	+4.6	64.8	+6.0	+0.9
M2	1250	45.2	+19.1	+5.2	48.6	+14.2	+5.8	77.0	+7.6	+1.4
	1350	35.2	+19.8	+3.7	47.2	+16.8	+6.6	76.8	+9.6	+2.1
	1450	31.3	+19.2	+2.4	38.9	+14.6	+4.1	71.0	+8.9	+0.6
M3	1350	39.6	+22.8	+4.1	41.8	+19.2	+4.8	69.9	+12.1	+0.8
M4	1350	40.9	+26.1	+4.8	58.2	+15.8	+3.6	80.8	+9.1	+0.4

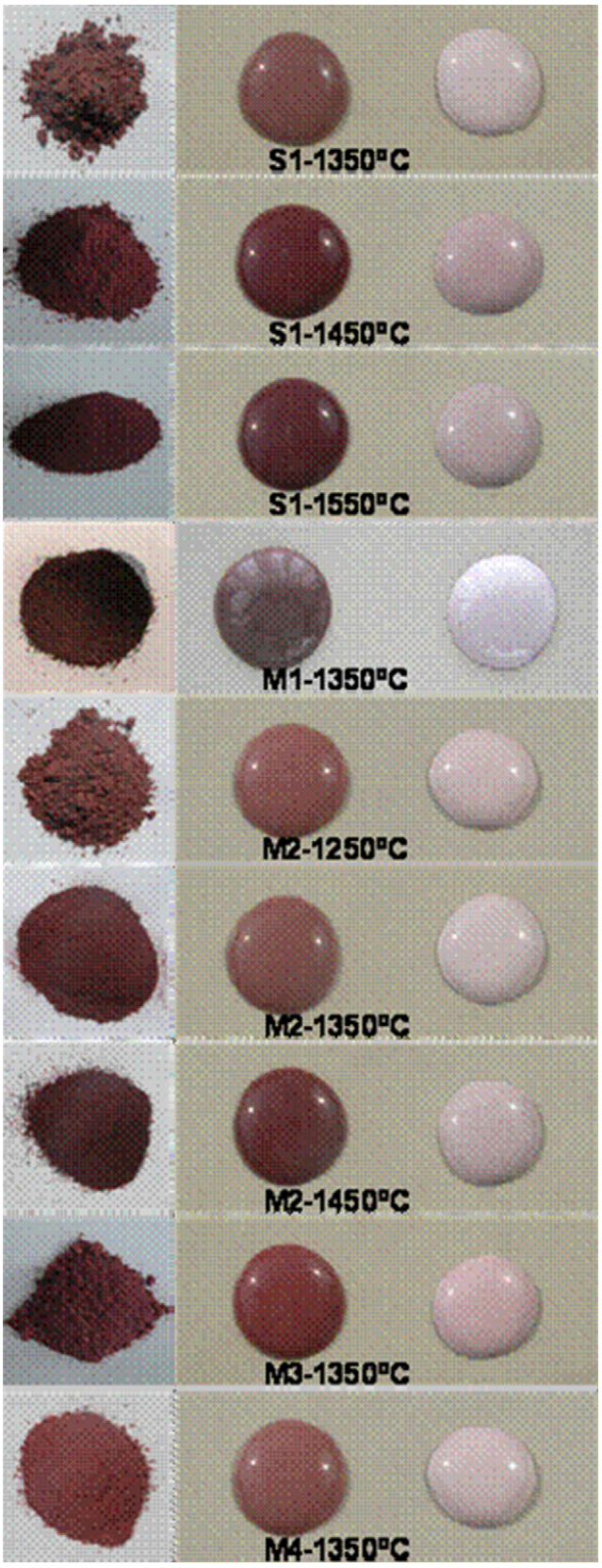

Fig. 7. Colours developed by the pure pigments (left) and colours of the transparent (centre) and opaque (right) glazes containing 5 wt% pigments. (For interpretation of the references to color in this figure legend, the reader is referred to the web version of this article.)

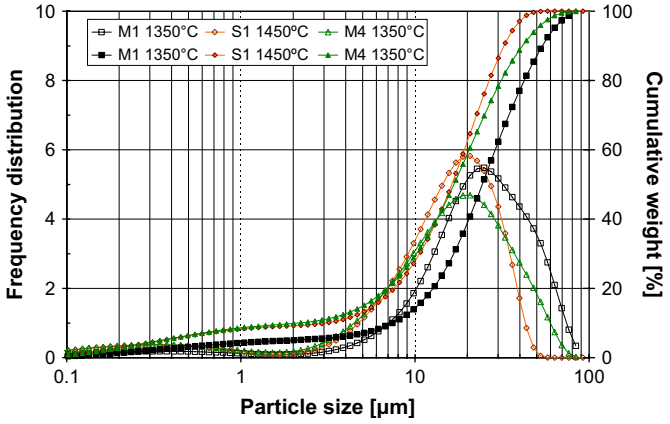

Fig. 8. Particle size distribution of some pigments in the as-used condition.

The optical spectra of sludge-bearing pigments are characterised by a light absorbance directly proportional to the amount of chromophore (Fig. 5). The reference malayaite exhibits a similar spectrum at high energies (>16,000 cm^{-1}) but some differences in the red-IR region. These spectra were successfully deconvolved considering different contributions by Cr^{4+} (accounting for the strong light absorptions at ~19,000 and ~25,000 cm^{-1}), Cr^{3+} (for its characteristic spin-forbidden transitions at ~13,000 and ~14,300 cm^{-1}) and Ni^{2+} (for the band at ~12,000 cm^{-1}, absent in the Ni-free reference malayaite). These assignments are consistent with literature [5,6] and Tanabe–Sugano diagrams for d^2 and d^3 electronic configurations (Cr^{4+} and Cr^{3+}, respectively) [19,20]. Resulting optical parameters for Cr^{3+} are $16{,}600 < \Delta_o < 17{,}100\ cm^{-1}$ (crystal field strength) and $420 < B < 510\ cm^{-1}$ (Racah interelectronic repulsion); for Cr^{4+} Δ_o is always close to 20,100 cm^{-1} while B is in the 630–680 cm^{-1} range. These data are in good agreement with crystal field theory [23]. The quantitative interpretation of optical spectra is coherent with pigment stoichiometry (Fig. 6): the larger the amount of Cr and Ni, the higher the band area of the main transitions. The Cr^{4+}/Cr^{3+} ratio was estimated on the basis of the spin-allowed transitions $^3T_{2g}(Cr^{4+})$ and $^4T_{2g}(Cr^{3+})$, whose band areas (Table 3) are more reliably deconvolved and less overlapped by charge transfer and Ni bands. It seems that the Cr^{4+}/Cr^{3+} ratio is very close in the samples S1 and M1 (Cr^{4+}/Cr^{3+} ~2.5) but it drops abruptly in M2 (1.7) to increase linearly by decreasing the chromium amount, being 2.0 in M3 and 3.1 in M4. The reason for this anomalous trend of the Cr^{4+}/Cr^{3+} ratio is not clear, but it could imply complex electric charge balance of the malayaite crystal lattice, involving other metals contained in the sludge (i.e. Ni, Zn). This observation may explain the colour differences, expressed in terms of L^*, a^*, b^* values, of sintered pigments (Table 4). Red-wine is the dominant hue and the pigment's brightness tends to decrease by increasing the calcination temperature (from 1250 to 1550 °C) due to progressive incorporation of the chromophore inside the malayaite lattice. Furthermore, a key role is likely to be played by the oxidation state of chromium and particularly the Cr^{4+}/Cr^{3+} ratio, as the

most important band affecting the colour is that of Cr^{4+} ($^3T_{2g}$ at ~19,000 cm^{-1}). As a matter of fact, the best red hue (a^* ~ 26) was achieved in the sample with the highest Cr^{4+}/Cr^{3+} ratio (i.e. M4). However, this effect is not observed in sample M1, even though it has a rather high Cr^{4+}/Cr^{3+} ratio, probably as a consequence of interference from Ni^{2+}, that is present in this pigment with the highest NiO/Cr_2O_3 molar ratio (4.66). By increasing the amount of Ni^{2+}, its band in the near IR gains intensity, increasing the absorbance in the red region of visible spectrum, so ''dirtying'' the magenta hue.

The value of red (a^*) colour coordinate is at its maximum at 1450 °C in the standard formulation, while is reached only at 1350 °C in the sludge-containing equivalent formulation. Waste impurities seem to exert a mineralising/fluxing action, increasing the reactivity of the mixture. This means that a similar colour is developed at lower processing temperature, therefore offering an obvious economical benefit [24].

Fig. 7 illustrates the colour of pigments in powder and dispersed into transparent and opaque glazes (fired at 1050 °C). The best colour developed by S1 and M (Gs-containing) pigments in both glazes is similar, but waste-containing pigments give slightly purer and brighter colours (see Table 4). Even if the purest red hue of pigment is reached with M4, this formulation (Cr_2O_3:$SnO_2 = 0.005$) tends to show less performance once applied on glazes, as the best a^* values are obtained with M3. The presence of nickel in the sludge seems not to cause deleterious chromatic changes and is also probably responsible for the higher colour purity of the sludge-containing pigments when compared with similar commercial ones.

The particle size distribution of some pigments in the as-used condition is given in Fig. 8. M4 tends to show a broader distribution and is constituted by coarser particles, suggesting that milling efficiency was lower than with S1 and M1 samples. Differences between these two pigments are very small. In all cases, a significative amount (>40 wt%) of particles coarser than 20 μm were detected.

4. Conclusions

Chrome-tin red malayaite − $Ca(Sn,Cr)SiO_5$ − containing a galvanizing sludge from the Cr/Ni plating process was successfully prepared by a common solid state reaction method, obtaining high-purity ceramic pigments (≥96% malayaite). The colour developed by these pigments, complying with standard expectations, is due to the occurrence of both Cr^{4+} and Cr^{3+} replacing Sn^{4+} in octahedral coordination. A variable Cr^{4+}/Cr^{3+} ratio was observed to affect significantly the red chromatic component (a^*).

Interesting colouring effects were obtained by adding the sludge-bearing pigments to transparent and opaque glazes, with a chromatic response equal or even better than that of commercial malayaite pigments. The best results are obtained by adding chromium to a maximum of 0.03 Cr_2O_3/SnO_2 molar ratio. Larger sludge additions imply an increased NiO content that interferes with chromium incorporation into the crystal lattice and optical properties. Although a complete evaluation of the stability limits is still required, it seems that the pigment hues remain fairly constant over a suitable temperature range.

Acknowledgement

The work was supported by FCT (Ph.D. grant of G. Costa).

References

[1] Muñoz R, Masó N, Júlian B, Márquez F, Beltrán H, Escribano P, et al. Environmental study of Cr_2O_3−Al_2O_3 green ceramic pigment synthesis. J Eur Ceram Soc 2004;24:2087−94.
[2] DCMA. Classification and chemical description of the mixed metal oxide inorganic coloured pigments. Metal Oxides and Ceramics Colors Subcommittee. 2nd ed. Washington, DC: Dry Color Manufacturer's Association; 1982.
[3] Papp JF. Chromite. Am Ceram Soc Bull 1995;74:118−20.
[4] Lopez-Navarrete E, Caballero A, Orera VM, Lázaro FJ, Ocaña M. Oxidation state and localization of chromium ions in Cr-doped cassiterite and Cr-doped malayaite. Acta Mater 2003;51:2371−81.
[5] Doménech A, Torres FJ, Ruiz de Sola E, Alarcón J. Electrochemical detection of high oxidation state of chromium (IV and V) in chromium-doped cassiterite and tin-sphene ceramic pigmenting systems. Eur J Inorg Chem 2006:638−48.
[6] Monrós G, Pinto H, Badenes J, Llusar M, Tena MA. Chromium(IV) stabilization in new ceramic matrices by coprecipitation method: application as ceramic pigments. Z Anorg Allg Chem 2005;631:2131−5.
[7] Heyns AM, Harden PM. Evidence for the existence of Cr(IV) in chromium-doped malayaite Cr^{4+}:$CaSnOSiO_4$: a resonance Raman study. J Phys Chem Solids 1999;60:277−84.
[8] Henderson B, Gallagher HG, Han TPJ, Scott MA. Optical spectroscopy and optimal crystal growth of some Cr^{4+}-doped garnets. J Phys Condens Matter 2000;12:1927−38.
[9] Hazenkamp MF, Güdel HU, Atanasov M, Kesper U, Reinen D. Optical spectroscopy of Cr^{4+}-doped Ca_2GeO_4 and Mg_2SiO_4. Phys Rev B 1996;53:2367−77.
[10] Bondioli F, Ferrari AM, Leonelli C, Manfredini T. Syntheses of Fe_2O_3/silica red inorganic inclusion pigments for ceramic applications. Mater Res Bull 1998;33:5−11.
[11] Marinova Y, Hohemberger JM, Cordoncillo E, Escribano P, Carda JB. Study of solid solutions, with perovskite structure, for application in the field of ceramic pigments. J Eur Ceram Soc 2003;23:213−20.
[12] Bondioli F, Barbieri L, Manfredini T. Grey ceramic pigment (Fe,Zn)Cr_2O_4 obtained from industrial fly-ash. Tile Brick Int 2000;16:246−8.
[13] Gomes V, Novaes de Oliveira AP, Labrincha JA. Ceramic pigment based on mullite structure obtained from Al-sludge containing formulations. Am Ceram Soc Bull 2005;84:9501−4.
[14] Ribeiro MJ, Tulyaganov DU, Labrincha JA, Ferreira JMF. Production of Al-rich sludge-containing bodies by different shaping techniques. J Mater Process Technol 2004;148:139−46.
[15] Costa G, Ribeiro MJ, Labrincha JA. Waste-based new ceramic pigments. Proceedings of fifth international congress valorisation and recycling of industrial waste. L'Aquila, Italy. CD: poster-paper no. 3; June 28th−July 1st 2005.
[16] Tilley R, editor. Colour and the optical properties of materials. England: John Wiley & Sons; 2000.
[17] Larson AC, Von Dreele RB. General structure analysis system (GSAS). Los Alamos National Laboratory Report, LAUR. 2000; p. 86−748.
[18] Toby HJ. EXPGUI, a graphical user interface for GSAS. J Appl Crystallogr 2001;34:210−3.
[19] Marfunin SA. Physics of minerals and inorganic materials. Berlin, Heidelberg, New York: Springer-Verlag; 1979.

[20] Lever ABP. Inorganic electronic spectroscopy. 2nd ed. Amsterdam: Elsevier; 1984.
[21] Magalhães JM, Silva JE, Castro FP, Labrincha JA. Physical and chemical characterisation of metal finishing industrial wastes. J Environ Manage 2005;75:157–66.
[22] Harisanov V, Pavlov RS, Marivova IT, Kozhukharov V, Carda JB. Influence of crystallinity on chromatic parameters of enamels coloured with malayaite pink pigment. J Eur Ceram Soc 2003;23: 429–35.
[23] Burns RG. Mineralogical applications of crystal field theory. 2nd ed. Cambridge University Press; 1993.
[24] Cordoncillo E, del Rio F, Carda J, Llusar M, Escribano P. Influence of some mineralizers in the synthesis of sphene-pink pigments. J Eur Ceram Soc 1998;18:1115–20.